



Supercurrent enhancement in Bloch domain walls

J. W. A. Robinson¹, F. Chiodi², M. Egilmez¹, Gábor B. Halász^{1,3} & M. G. Blamire¹

¹Department of Materials Science and Metallurgy, University of Cambridge, Pembroke Street, Cambridge, CB2 3QZ, United Kingdom, ²Institut d'Electronique Fondamentale, Université Paris-Sud, bât 220, 91405 Orsay cedex, France, ³Theoretical Physics, Oxford University, 1 Keble Road, Oxford OX1 3NP, United Kingdom.

SUBJECT AREAS:
NANOTECHNOLOGY
QUANTUM PHYSICS
SUPERCONDUCTIVITY
MAGNETIC MATERIALS AND
DEVICES

Received
1 March 2012

Accepted
3 September 2012

Published
26 September 2012

Correspondence and
requests for materials
should be addressed to
J.W.A.R. (jjr33@cam.
ac.uk)

Conventional spin-singlet Cooper pairs convert into spin-triplet pairs in ferromagnetic Josephson junctions in which the superconductor/ferromagnet interfaces (S/F) are magnetically inhomogeneous. Although much of the theoretical work describing this triplet proximity effect has considered ideal junctions with magnetic domain walls (DW) at the interfaces, in practice it is not easily possible to isolate a DW and propagate a supercurrent through it. The rare-earth magnet Gd can form a field-tuneable in-plane Bloch DW if grown between non-co-linearly aligned ferromagnets. Here we report supercurrents through magnetic Ni-Gd-Ni nanopillars: by field annealing at room temperature, we are able to modify the low temperature DW-state in Gd and this result has a striking effect on the junction supercurrent at 4.2 K. We argue that this result can only be explained in terms of the interconversion of triplet and singlet pairs, the efficiency of which depends on the magnetic helicity of the structure.

Supercurrents in ferromagnetic Josephson junctions are strongly suppressed unless the superconductor/ferromagnet (S/F) interfaces are magnetically inhomogeneous so that conventional singlet Cooper pairs can convert into spin-aligned triplet pairs and vice-versa^{1,2}. Evidence for triplet-induced superconductivity in S-F hybrids was first reported more than ten years ago^{3,4}, predating the experimental proof of Josephson singlet P-coupling in S-F-S Josephson junctions (see, e.g., Ref. 5–17). A few years later, supercurrents in Josephson junctions with half-metallic ferromagnetic CrO₂ barriers were also reported¹⁸. These pioneering experiments had relatively low reproducibility because the S/F interfaces relied on the spontaneous appearance of inhomogeneous magnetic states to generate triplet pairs. Recently, however, a series of experiments have been reported that demonstrate triplet pair supercurrent creation in S-F-S junctions by engineering the S/F interfaces to be magnetically inhomogeneous^{19–25}. See also related works reporting evidence of induced triplet superconductivity using scanning tunnelling spectroscopy on S-F bilayers^{26,27}, conductance measurements and Andreev spectroscopy in S-F junctions^{28–31}, and critical temperature measurements of S-F spin-valves³².

Due to the intrinsic magnetic inhomogeneity, a magnetic domain wall (DW) at an S/F interface should theoretically be an ideal triplet pair generator (see, e.g., Refs. 1 and 33–35). In most ferromagnets, however, the DW density even at the coercive field is not large enough to have a significant effect on the Josephson current of an S-F-S junction. This means that it is practically impossible to probe the effect that DWs have on the supercurrents that pass through them. As an alternative, intrinsically DW-like ferromagnets such as Ho can be used³⁶ and indeed our group^{20,37} (see also Ref. 38) and Sosnin *et al.*¹⁹ have demonstrated results consistent with a triplet proximity effect in Ho-based junctions. Nevertheless, due to its high intrinsic anisotropy and interlayer exchange coupling energies it is not possible to unwind the helimagnetic structure without applying large (typically larger than 4 T) magnetic fields during transport measurements that would strongly suppress the superconductivity and any Josephson current in the superconductors studied; this makes it impossible to study directly how the magnetic structure controls the resultant supercurrent. A proper test for the role of DWs in mediating supercurrents requires therefore a magnetic structure in which the DW can be modified through magnetic field history.

Exchange coupling at the interface between rare earth (RE) and transition metal (TM) ferromagnets results in an equilibrium antiparallel alignment of their moments. Non-parallel alignment of the TM layer moments in a TM-RE-TM trilayer can result in an in-plane Bloch DW in the RE³⁹ which can be modified by changing the alignment of the TM layers. Here we report supercurrents in Nb-Ni-Gd-Ni-Nb nanopillar Josephson junctions: depending on the Gd thickness, magnetic field annealing can significantly reduce the net barrier moment and substantially increase the junction supercurrent.

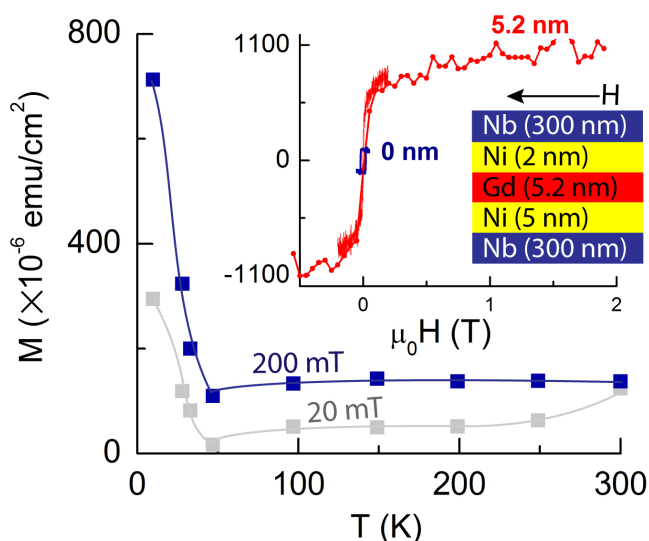


Figure 1 | Field-cooled temperature dependence of the magnetic moment per unit area for an unpatterned Nb(300 nm)-Ni(5 nm)-Gd(5.2 nm)-Ni(2 nm)-Nb(300 nm) film. The magnetic fields were applied in-plane as shown by the illustration. The inset shows the magnetic moment per unit area versus in-plane magnetic field for the same film at 9.8 K and comparative data from a Nb-Ni-Nb film at 100 K with a Ni thickness of 7 nm. Solid lines are a guide to the eye.

It has been shown previously that for barriers consisting of two ferromagnetic layers, parallel and antiparallel alignments of the layer moments result in different critical currents^{40,41}. Since the magnetism in that case is always co-linear (i.e., there is no inhomogeneity of the form necessary to initiate spin-aligned triplet pairing), the larger critical current observed for antiparallel alignment originates from the “unwinding” of the singlet pair dephasing. We will show later that this effect cannot explain the observations reported here.

Results

Magnetic properties. For our experiment, a series of samples were prepared with different Gd thicknesses (d_{Gd}) between 1.1 nm and 5.2 nm. The top and bottom Nb layers were both 300-nm-thick, and the top and bottom Ni layers had thicknesses 2 nm and 5 nm, respectively. Figure 1 shows the field-cooled temperature dependence of the magnetic moment per unit area for an unpatterned Nb-Ni-Gd-Ni-Nb film with a 5.2-nm-thick Gd layer, measured using a vibrating sample magnetometer in which the field was applied in-plane as shown. The data shows a compensation point near 50 K where the moments of the antiparallel-aligned Ni and Gd are equal. Results for other Gd thicknesses are similar. A similar compensation point was reported by Barth *et al.* for Ni-Gd bilayers⁴².

Nanopillar Josephson junction characteristics. Nanopillar Nb-Ni-Gd-Ni-Nb Josephson junctions were fabricated using a focused ion beam technique (see Methods Section and Refs. 43 and 44 for further information). Electrical measurements on junctions in a four-point current-biased configuration were performed using a magnetically-shielded dip-stick probe in a liquid He dewar. Current-voltage (IV) curves were measured with a lock-in amplifier from which the normal state resistance (R_N) of a junction was measured at high voltage with a well-defined noise error.

To confirm a Josephson effect in these junctions, we measured the effect of an in-plane magnetic field (H) on a junction’s critical current (I_C). Fraunhofer-like oscillations of the critical current were obtained in all junctions, as shown in Fig. 2. The $I_C(H)$ curves are hysteretic in magnetic field. This is because the total flux within the junction is the sum of that due to the applied field and the intrinsic flux generated by

the net magnetisation (M_T) of the composite Ni-Gd-Ni barrier. For the simple case in which M_T follows a square hysteresis loop, the relative field-shift (ΔH) in $I_C(H)$ is given by αM_T , where α is a geometric flux-coupling factor. In other words, the maximum critical current (I_{Max}) is offset by a finite field $\pm \Delta H$ that is proportional to the net magnetisation of the barrier.

The $I_C(H)$ patterns of all junctions were measured in three stages. Stage 1 was the virgin state in which no magnetic field was applied to the junction before cooling down to 4.2 K [Fig. 2(i)]. For stage 2 the junctions were warmed to room temperature and a 0.1 T magnetic field was applied in-plane. After switching off the field, the junctions were cooled to 4.2 K and $I_C(H)$ was re-measured [Fig. 2(ii)]. Finally (Stage 3), the junctions were warmed to room temperature and a 1.0 T magnetic field was applied in-plane. After switching off the field, the junctions were cooled to 4.2 K and $I_C(H)$ was re-measured [Fig. 2(iii)].

From Fig. 2 it can be seen that, with exception of the $d_{\text{Gd}} = 1.1$ nm data, ΔH and I_{Max} in the Fraunhofer field patterns are dramatically changed by the room temperature field treatment where, for progressively larger applied fields, I_{Max} increases and ΔH decreases. This is more clearly shown in Fig. 3(a) – 3(d) where we plot the relation between I_{Max} and ΔH for a number of different devices for each Gd thickness (to compare junctions with different cross-sectional areas and Gd thicknesses, I_{Max} was multiplied by R_N to give the maximum characteristic voltage $I_{\text{Max}}R_N$ as a function of ΔH). In Fig. 3(e) we show the dependence of the average maximum and minimum values of $I_{\text{Max}}R_N$ as a function of Gd thickness.

In nanopillar devices in which the barrier is a single ferromagnetic layer, the value of ΔH implies that the barrier is single domain²⁰. For the Ni-Gd-Ni devices reported here, ΔH is dependent on magnetic history and so must have a more complicated magnetic structure reflecting a competition between the exchange coupling within the Ni and Gd layers, the interlayer exchange coupling, the magnetostatic coupling between the layers, and the magnetic history of the samples. In the unpatterned films, the magnetostatic coupling is small compared to the various exchange energies and at low temperatures these exchange energies are minimised when the angle between the Ni layers (θ) is zero and the Gd is homogeneously magnetised in the opposite direction. The compensation point in the data of Fig. 1 demonstrates this; henceforth this magnetic structure is referred to as the co-linear ferrimagnetic configuration. In the patterned nanopillars, the magnetostatic energy associated with the fringing fields is significant⁴⁵: at high temperatures where the Gd is non-magnetic, this favors $\theta = 180^\circ$. However, at low temperatures, the cross-coupling between the Ni and Gd layers adds an additional exchange energy which acts to destabilise this arrangement.

Here we focus on the formation of an in-plane Bloch DW in Gd as a means of reducing the magnetostatic energy [see Fig. 4]. It was shown earlier³⁹ that the energy of a DW in such structures is modified by the antiferromagnetic exchange interaction between transition-metals and Gd. Experimentally it was demonstrated that in micrometre-scale Py-Gd-Py (permalloy, $\text{Ni}_{80}\text{Fe}_{20}$) trilayer mesas the magnetostatic energy is eliminated through the formation of a 180° in-plane DW within the Gd layer even for Gd thicknesses as small as 2 nm, which enabled the 100-nm-thick Py layers to align antiparallel³⁹. The Ni layers are much thinner in our devices than in those in Ref. 39, but the nanopillar dimensions are correspondingly smaller and so the magnetostatic energy remains substantial relative to the exchange energy. This suggests that, with increasing Gd thickness, there should be a crossover from the co-linear ferrimagnetic state to one in which a Gd DW is nucleated to reduce the magnetostatic energy.

We now present a general expression for ΔH (d_{Gd}) in a Ni-Gd-Ni nanopillar barrier with and without an in-plane DW in Gd. To accommodate the misalignment between the Ni layers, we assume that the Gd magnetisation is perfectly helical, i.e. the in-plane magnetisation angle $\varphi(z)$ varies linearly along the junction axis z (orthogonal to

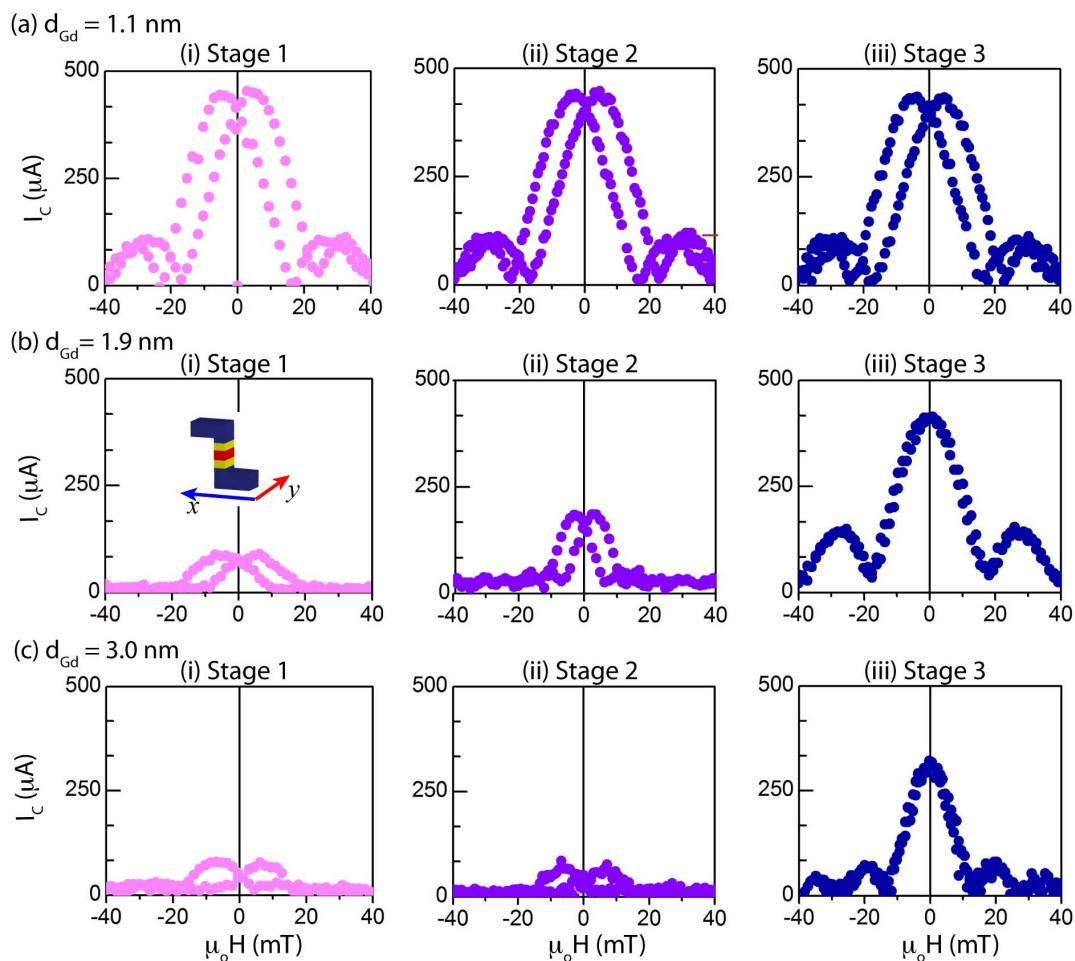


Figure 2 | Critical current modulation of Nb-Ni-Gd-Ni-Nb junctions. (a–c) Fraunhofer patterns at 4.2 K for samples with different Gd thicknesses (d_{Gd}) at stages 1, 2, and 3, as described in the main text. The magnetic field was applied parallel to x [see inset in (b)(i)] except in (b)(ii) where the field was applied parallel to y.

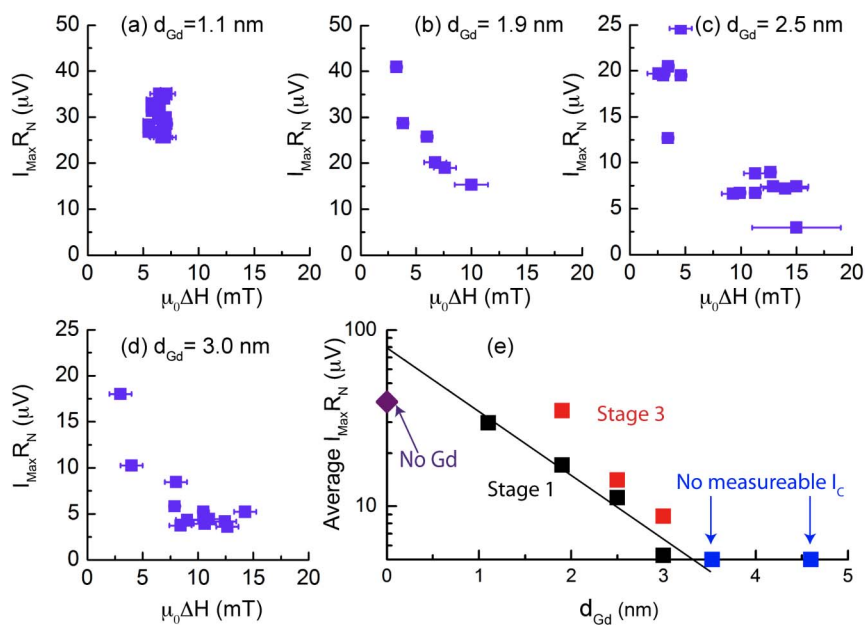


Figure 3 | Supercurrent dependence of Nb-Ni-Gd-Ni-Nb junctions at 4.2 K. (a–d) The dependence of the $I_{\text{Max}}R_{\text{N}}$ product on the net intrinsic field of the Ni-Gd-Ni barriers for samples with different Gd spacer thickness; (e) The average minimum and average maximum values of $I_{\text{Max}}R_{\text{N}}$ versus Gd thickness measured at stages 1 and 3 respectively; the arrowed squares represent thicknesses at which no supercurrent was measurable.

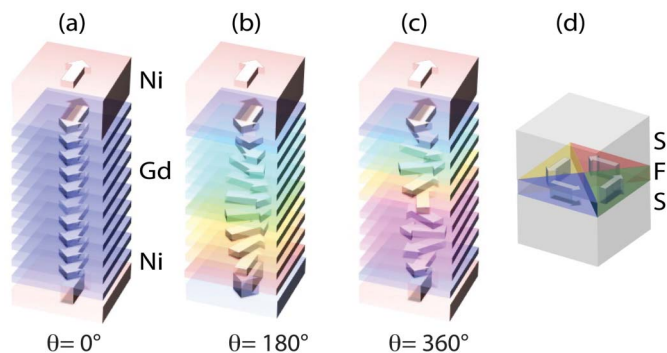


Figure 4 | Possible low temperature magnetic configurations of Nb-Ni-Gd-Ni-Nb nanopillar junctions. (a) A co-linear ferrimagnetic Ni-Gd-Ni trilayer structure. (b) Antiparallel Ni layers with Gd forming an in-plane 180° Bloch domain wall. (c) Parallel Ni layers with Gd forming an in-plane 360° Bloch domain wall. (d) An in-plane flux-closed configuration.

the layer interfaces). The shift, ΔH , in the Fraunhofer pattern is proportional to the net moment which is then given by:

$$\Delta H \propto$$

$$\sqrt{\left[(d_{Ni,1} - d_{Ni,2}) \sin \frac{\theta}{2} \right]^2 + \left[(d_{Ni,1} + d_{Ni,2}) \cos \frac{\theta}{2} - 2\gamma d_{Gd} \frac{\sin(\theta/2)}{\theta} \right]^2}, \quad (1)$$

where $\gamma = M_{Gd} / M_{Ni}$. From the magnetisation data in Fig. 1, we estimate γ to be approximately 10.

In Fig. 5, we have plotted theoretical values of $\Delta H(d_{Gd})$ on Gd thickness from Eq. (1) for three different values of θ , together with the average maximum and minimum values of ΔH obtained from the $I_C(H)$ measurements. The constant of proportionality in Eq. (1) is

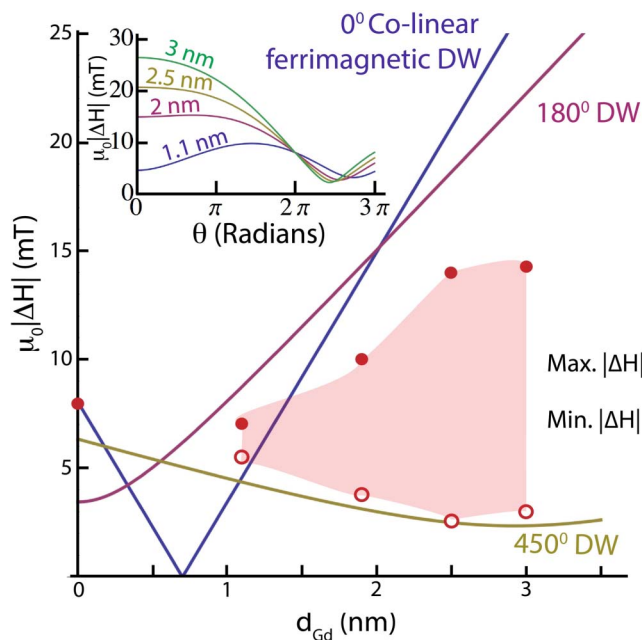


Figure 5 | Intrinsic field of nanopillar Nb-Ni-Gd-Ni-Nb junctions at 4.2 K. The solid curves show the theoretical dependence of ΔH from Eq. (1) on Gd thickness for different Bloch domain wall (DW) angles. The filled and hollow data represent the maximum and minimum values of ΔH obtained from the $I_C(H)$ measurements shown in Fig. 2 while the shaded region represents the spread in ΔH . (Inset) The theoretical dependence of ΔH on DW angle for different Gd thicknesses.

chosen in such a way that the co-linear ferrimagnetic curve coincides with the data point at $d_{Gd} = 0$. No other fitting parameter is used.

The co-linear ferrimagnetic curve passes near the $d_{Gd} = 1.1$ nm data point, which is in agreement with our initial assumption that for small Gd thicknesses it is energetically unfavourable to nucleate a DW. For $d_{Gd} > 1.1$ nm, the largest measured values of ΔH are closer to the 180° DW curve than the co-linear ferrimagnetic curve, implying the formation of a DW for these samples. Following high field annealing, the data points for $d_{Gd} > 1.1$ nm lie close to the curve corresponding to a 450° DW. As shown in the inset to Fig. 5, the minimum barrier flux occurs around this angle and so this configuration has a minimum magnetostatic energy. Clearly this structure has a much larger magnetic inhomogeneity so this, within a triplet picture, is consistent with the enhanced critical current.

We know of no way of experimentally confirming these magnetic configurations in isolated nanopillar devices. However, we believe that sufficient supporting information exists to make the DW scenario plausible. Firstly, it has been confirmed both magnetically and electrically that a DW can be nucleated in Gd layer as thin as 2 nm³⁹. Secondly, the fact that the barrier magnetism can be changed by magnetic annealing implies that the Ni magnetisation is irreversible at room temperature (RT) even in the absence of a significant exchange interaction with the Gd: applying progressively larger fields must make this RT state closer to $\theta = 0$, while the virgin state is likely to be closer to $\theta = 180^\circ$ to minimise the magnetostatic energy. Finally, on cooling through the Curie temperature of Gd, various DW angles can be nucleated from a given starting value of θ : for example, for $\theta = 0$, either a co-linear ferrimagnetic configuration or a 360° DW could form. As shown in the inset to Fig. 5, the latter has a much lower moment (and hence magnetostatic energy) for larger Gd thicknesses, and the moment can be further reduced by a relaxation to a DW angle greater than 360° .

Discussion

The analysis above provides a direct link between the rotation angle of the internal DW (as measured by ΔH) and the I_C . Before we can draw any conclusions regarding the role of unconventional superconductivity in the behaviour, it is important to eliminate a rather trivial effect of flux in controlling the critical current via the standard Josephson relation $I_J = I_0 \sin \phi$, where ϕ is the local phase-difference across the barrier. For a square magnetic hysteresis loop, a net barrier flux gives rise to a standard Fraunhofer pattern with an offset ΔH which reverses at the coercive field. The important aspect of this is that the maximum critical current corresponding to the complete cancellation of the barrier flux by the magnetic field is identical to I_0 .

This cancellation is possible only because the barrier magnetisation is laterally homogeneous. For inhomogeneous magnetisation, such as in-plane flux closure structures of the type illustrated in Fig. 4(d), the applied field cannot eliminate a phase variation across the junction and hence $I_{Max} < I_0$; this has been experimentally demonstrated in much larger junctions than ours⁴⁶. This argument can be extended to barriers consisting of exchange-coupled magnetic multilayers of the type considered here. The conclusion is that the lateral magnetic inhomogeneity associated with the in-plane flux closure results in a suppression of the maximum critical current with respect to the non-magnetic or single-domain magnetic states: in other words, a dependence of I_{Max} on ΔH which is opposite to that observed here.

We now consider the configuration which we have proposed for our devices, in which an in-plane DW lies in the Gd layer [see Figs. 4(b) and 4(c)]. Provided that each atomic layer remains single-domain, the net magnetisation vector integrated normal to the plane of the junction is independent of position and can be cancelled by the appropriate applied field. Therefore, the maximum critical current should be independent of the net magnetic moment and so cannot account for the dependence reported here.



As noted in the introduction, it is also important to consider the possibility that the relative alignment of the Ni layers controls a singlet supercurrent. For example, in Ref. 41 it was shown that for a Nb-Py-Cu-Co-Nb junction in which an applied field could be used to control the relative orientations of the magnetisations of the magnetic layers, a much larger critical current was obtained when the Py ($\text{Ni}_{80}\text{Fe}_{20}$) and Co layers were antiparallel. A similar result was obtained in a related experiment with Fe-Cr-Fe barriers in which the Cr spacer layer thickness controlled the relative magnetisation directions of the Fe layers⁴⁰; theoretical fits demonstrated that this result was consistent with the conventional singlet proximity effect.

In the experiments reported here, the relative alignment of the Ni layers is altered by the magnetic history. However, it is obvious from Fig. 5 that the configuration in which the Ni layers are antiparallel ($\theta = 180^\circ$) has a large net moment (mainly originating from the Gd) which corresponds to the minimum rather than the maximum critical current. In fact the configuration which corresponds to the maximum critical current for $d_{\text{Gd}} > 1.1$ nm is closer to parallel alignment of the Ni layers.

In Fig. 3(e) we have plotted the dependence of the average normalised supercurrent on the Gd thickness. There are several important points to be made about this figure. Firstly, for both the maximum and minimum values of the supercurrent, there is a strong reduction with increasing Gd thickness, reflecting the short mean free path of Gd which translates into a short coherence length for both singlet and triplet pairs. Nevertheless, the supercurrent for the 1.9 nm thickness data is higher than that for 1.1 nm and comparable with the pure Ni sample with no Gd.

The conclusion is therefore that the significant enhancement in the maximum critical current with a reduction in ΔH that we see in our results cannot be due to an incomplete flux cancellation or due to a conventional singlet proximity effect. Nevertheless, the experimental results demonstrate that the junction supercurrent is directly dependent on the magnetic structure in the Gd layer. Our analysis shows that the supercurrent increases with the angle between the Ni layers and hence depends on the helicity of the in-plane DW in the Gd layer. Theoretically, in such S-F-F²-F-S junctions, spin-aligned triplet pairs form via a spin-mixing effect⁴⁷. This means that the supercurrent cannot be understood purely in terms of simple singlet Cooper pair phase-shifts. We argue that the magnetic structure in Gd is a Bloch DW, and Eschrig *et al.* in Ref. 33 have shown theoretically that in the diffusive limit there is an inter-conversion between singlet and triplet pairs at the F/DW interfaces (i.e., equivalent to the Ni/Gd interfaces in our experiment). The generation of triplet pairs necessarily means that the Josephson effect is enhanced and so the junction critical current increases. Our results are consistent with this picture and the increase in the junction supercurrent with increasing DW-angle in Gd implies an increasing efficiency in the conversion between singlet and triplet pairs.

Methods

Growth of multilayer thin-films. Nb-Ni-Gd-Ni-Nb thin-films were grown using d.c.-magnetron sputtering in an Ar plasma at 1.5 Pa onto 10×4 mm² and 4×4 mm² unheated single crystal silicon substrates with a 250-nm-thick oxide layer on the surface. Prior to film growth and during the deposition, the walls of the main chamber of the system were cooled via a liquid nitrogen jacket to lower the system's base pressure to below 10^{-8} Pa (verified using an in-situ residual gas analyser). Substrates rested on a circular table that rotated below stationary sputtering targets. All targets were pre-sputtered until a constant and stable voltage was achieved (typically between 10 and 15 minutes). The film growth rate was controlled by the target power and the speed in which the substrates passed below the stationary targets. Deposition rates and film thicknesses were pre-calibrated using atomic force microscopy to measure pre-deposited step-edges.

Nanopillar device fabrication. Films were patterned by standard optical lithography and Ar-ion milling to produce a series of 4- μm -wide and 30- μm -long wires, each connected to four larger area contact pads to allow for four-point measurements to be performed. Within each wire a nanopillar Josephson junction was processed using a focused Ga-ion beam microscope technique. We have described this process in detail

elsewhere in Refs. 43 and 44. The junction areas were approximately square and in the 300×300 nm² to 1200×1200 nm² range.

- Bergeret, F. S., Bergeret, F. S., Volkov, A. F. & Efetov, K. B. Odd triplet superconductivity and related phenomena in superconductor-ferromagnet structures. *Rev. Mod. Phys.* **77**, 1321–1373 (2005).
- Bergeret, F. S., Volkov, A. F. & Efetov, K. B. Long-range proximity effects in superconductor-ferromagnet structures. *Phys. Rev. Lett.* **86**, 4096–4099 (2001).
- Petrashov, V. T., Sosnin, I. A., Cox, I., Parsons, A. & Troadec, C. Giant mutual proximity effects in ferromagnetic/superconducting nanostructures. *Phys. Rev. Lett.* **83**, 3281–3284 (1999).
- Giroud, M., Courtois, H., Hasselbach, K., Mailly, D. & Pannetier, B. Superconducting proximity effect in a mesoscopic ferromagnetic wire. *Phys. Rev. B* **58**, R11872–R11875 (1998).
- Ryazanov, V. V. *et al.* Coupling of two superconductors through a ferromagnet: Evidence for a pi junction. *Phys. Rev. Lett.* **86**, 2427–2430 (2001).
- Kontos, T., Apili, M., Lesueur, & Grison, X. Inhomogeneous superconductivity induced in a ferromagnet by proximity effect. *Phys. Rev. Lett.* **86**, 304–307 (2001).
- Blum, Y., Tsukernik, A., Karpovskii, M. & Palevski, A. Oscillations of the superconducting critical current in Nb-Cu-Ni-Cu-Nb junctions. *Phys. Rev. Lett.* **89**, 187004 (2002).
- Sellier, H., Baraduc, C., Lefloch, F. & Calemczuk, R. Half-Integer Shapiro Steps at the 0-Pi Crossover of a Ferromagnetic Josephson Junction. *Phys. Rev. Lett.* **92**, 257005 (2004).
- Bell, C., Loloee, R., Burnell, G. & Blamire, M. G. Characteristics of strong ferromagnetic Josephson junctions with epitaxial barriers. *Phys. Rev. B* **71**, 180501 (2005).
- Robinson, J. W. A., Piano, S., Burnell, G., Bell, C. & Blamire, M. G. Critical current oscillations in strong ferromagnetic pi junctions. *Phys. Rev. Lett.* **97**, 177003 (2006).
- Oboznov, V. A., Bol'ginov, V. V., Feofanov, A. K., Ryazanov, V. V. & Buzdin, A. I. Thickness Dependence of the Josephson Ground States of Superconductor-Ferromagnet-Superconductor Junctions. *Phys. Rev. Lett.* **96**, 197003 (2006).
- Weides, M., Kemmler, M., Kohlstedt, H., Waser, R., Koelle, D., Kleiner, R. & Goldobin, E. 0-Pi Josephson Tunnel Junctions with Ferromagnetic Barrier. *Phys. Rev. Lett.* **97**, 247001 (2006).
- Robinson, J. W. A., Piano, S., Burnell, G., Bell, C. & Blamire, M. G. Zero to Pi transition in superconductor-ferromagnet-superconductor junctions. *Phys. Rev. B* **76**, 094522 (2007).
- Bannykh, A. A., Pfeiffer, Stolyarov, V. S., Batov, I. E., Ryazanov, V. V. & Weides, M. Josephson tunnel junctions with a strong ferromagnetic interlayer. *Phys. Rev. B* **79**, 054501 (2009).
- Robinson, J. W. A., Barber, Z. H. & Blamire, M. G. Strong ferromagnetic Josephson devices with optimized magnetism. *Appl. Phys. Lett.* **95**, 192509 (2009).
- Khaire, T. S., Pratt, W. P., Jr. & Birge, N. Critical current behavior in Josephson junctions with the weak ferromagnet PdNi. *Phys. Rev. B* **79**, 094523 (2006).
- Khasawneh, M., Pratt, W. P., Jr. & Birge, N. Josephson junctions with a synthetic antiferromagnetic interlayer. *Phys. Rev. B* **80**, 02506(R) (2009).
- Keizer, R. S., Goennenwein, S. T. B., Klapwijk, T. M., Miao, G. X., Xiao, G. & Gupta, A. A spin triplet supercurrent through the half-metallic ferromagnet CrO₂. *Nature* **439**, 825–827 (2006).
- Sosnin, I., Cho, H., Petrashov, V. T. & Volkov, A. F. Superconducting phase coherent electron transport in proximity conical ferromagnets. *Phys. Rev. Lett.* **96**, 157002 (2006).
- Robinson, J. W. A., Witt, J. D. S. & Blamire, M. G. Controlled Injection of Spin-Triplet Supercurrents into a Strong Ferromagnet. *Science* **329**, 59–61 (2010).
- Sprungmann, D., Westerholt, K., Zabel, H., Weides, M. & Kohlstedt, H. Evidence for triplet superconductivity in Josephson junctions with barriers of the ferromagnetic Heusler alloy Cu₂MnAl. *Phys. Rev. B* **82**, 060505(R) (2010).
- Khaire, T. S., Khasawneh, M. A., Pratt, W. P., Jr. & Birge, N. O. Observation of Spin-Triplet Superconductivity in Co-Based Josephson Junctions. *Phys. Rev. Lett.* **104**, 137002 (2010).
- Anwar, M. S., Czeschka, F., Hesselberth, M., Porcu, M. & Aarts, J. Long range spin supercurrents in ferromagnetic CrO₂ using a multilayer contact structure. *Phys. Rev. B* **82**, 100501 (2011).
- Anwar, M. S., Veldhorst, M., Brinkman, A. & Aarts, J. Long range supercurrents in ferromagnetic CrO₂ using a multilayer contact structure. *Appl. Phys. Lett.* **100**, 052602 (2012).
- Klose, C. *et al.* Optimization of Spin-Triplet Supercurrent in Ferromagnetic Josephson Junctions. *Phys. Rev. Lett.* **108**, 127002 (2012).
- Kalcheim, Y., Kirzhner, Koren, G. & Millo, O. Long-range proximity effect in La_{2/3}Ca_{1/3}MnO₃/(100)YBa₂Cu₃O_{7- δ} ferromagnet/superconductor bilayers: Evidence for induced triplet superconductivity in the ferromagnet. *Phys. Rev. B* **83**, 064510 (2012).
- Kalcheim, Y., Millo, O., Egilmez, M., Robinson, J. W. A. & Blamire, M. G. Evidence for anisotropic triplet superconductor order parameter in half-metallic ferromagnetic La_{0.7}Ca_{0.3}Mn₃O proximity coupled to superconducting Pr_{1.85}Ce_{0.15}CuO₄. *Phys. Rev. B* **85**, 104504 (2012).
- Almog, B., Hacohen-Gourgy, S., Tsukernik, A. & Deutscher, G. Long-range odd triplet order parameter with equal spin pairing in diffusive Co/In contacts. *Phys. Rev. B* **80**, 220512 (2009).



29. Hacothen-Gourgy, S., Almog, B. & Deutscher, G. Coexistence of a triplet nodal order parameter and a singlet order parameter at the interfaces of ferromagnet/superconductor Co/CoO/In junctions. *Phys. Rev. B* **84**, 014532 (2011).
30. Almog, B., Hacothen-Gourgy, S., Tsukernik, A. & Deutscher, G. Triplet order parameter component at Co/CoO/In contacts. *Phys. Rev. B* **84**, 054514 (2011)
31. Visani, C. *et al.* Equal-spin Andreev reflection and long-range coherent transport in high-temperature superconductor/half-metallic ferromagnet junction. *Nat. Phys.* **8**, 539 (2012).
32. Leksin, P. V., Garif'yanov, N. N., Garifullin, I. A., Fominov, Y. V., Schumann, J., Krupskaya, Y., Kataev, V., Schmidt, O. G. & Büchner, B. Evidence for Triplet Superconductivity in a Superconductor-Ferromagnet Spin Valve. *Phys. Rev. Lett.* **109**, 057005 (2012).
33. Eschrig, M., Kopu, J. Singlet-triplet mixing in superconductor-ferromagnet hybrid devices. *Advances in Solid State Physics* **44**, 533–545 (2004).
34. Fominov, Y. V., Fominov, Y. V., Volkov, A. F. & Efetov, K. B. Josephson effect due to the long-range odd-frequency triplet superconductivity in SFS junctions with Neel domain walls. *Phys. Rev. B* **75**, 104509 (2007).
35. Buzdin, A. I., Mel'nikov, A. S. & Pugach, N. G. Domain walls and long-range triplet correlations in SFS Josephson junctions. *Phys. Rev. B* **83**, 144515 (2011).
36. Witt, J. D. S., Hase, T. P. A., Fan, R., Kinane, C. J., Charlton, T. R., Langridge, S. & Blamire, M. G. Strain dependent selection of spin-slip phases in sputter deposited thin-film epitaxial holmium. *J. Phys. Condens. Matter* **23** 416006 (2011).
37. Usman, I. T. M. *et al.* Evidence for spin mixing in holmium thin film and crystal samples. *Phys. Rev. B* **83**, 144518 (2011).
38. Witt, J. D. S., Robinson, J. W. A. & Blamire, M. G. Josephson junctions incorporating a conical magnetic holmium interlayer. *Phys. Rev. B* **85**, 184526 (2012).
39. Prieto, J., Blamire, M. G. & Evetts, J. Magnetoresistance in a constricted domain wall. *Phys. Rev. Lett.* **90**, 027201 (2003).
40. Robinson, J. W. A., Halasz, G. B., Buzdin, A. I. & Blamire, M. G. Enhanced Supercurrents in Josephson Junctions Containing Nonparallel Ferromagnetic Domains. *Phys. Rev. Lett.* **104**, 207001 (2010).
41. Bell, C., Burnell, G., Leung, CW, Tarte, E. J. Kang, D. J. & Blamire, M. G. Controllable Josephson current through a pseudospin-valve structure. *Appl. Phys. Lett.* **84**, 1153 (2004).
42. Barth, A. *et al.* Magnetic coupling in Gd/Ni bilayers. *J. Phys. Condens. Matter* **20**, 395232 (2008).
43. Bell, C. *et al.* Fabrication of nanoscale heterostructure devices with a focused ion beam microscope. *Nanotechnology* **14**, 630–632 (2003).
44. Blamire, M. G., Aziz, A. & Robinson, J. W. A. Nanopillar junctions. *Phil. Trans. Roy. Soc. Math. Phys. Eng. Sci.* **369**, 3198–3213 (2011).
45. Aziz, A., Wessely, O. P., Ali, M., Edwards, D. M., Marrows, C. H., Hickey, B. J. & Blamire, M. G. Nonlinear Giant Magnetoresistance in Dual Spin Valves. *Phys. Rev. Lett.* **103**, 237203 (2009).
46. Weides, M. Magnetic anisotropy in ferromagnetic Josephson junctions. *Appl. Phys. Lett.* **93**, 052502 (2008).
47. Houzet, M. & Buzdin, A. I. Spin-triplet supercurrent through ferromagnetic trilayer. *Phys. Rev. B* **76**, 060504(R) (2007).

Acknowledgements

We are grateful to J. Linder for helpful comments. The work was funded by the Royal Society and the UK Engineering and Physical Sciences Research Council.

Author contributions

JWAR made the junctions and performed the superconducting measurements. He also designed the experiment and with MGB analysed the data and wrote the paper. FC performed the magnetic measurements with the help of ME, she also helped in the analysis of the data and participated in writing the paper. GBH performed theoretical calculations that were used to interpret the results. All authors reviewed the manuscript.

Additional information

Competing financial interests: The authors declare no competing financial interests.

License: This work is licensed under a Creative Commons Attribution-NonCommercial-NoDerivs 3.0 Unported License. To view a copy of this license, visit <http://creativecommons.org/licenses/by-nc-nd/3.0/>

How to cite this article: Robinson, J.W.A., Chiodi, F., Egilmez, M., Halász, G.B. & Blamire, M.G. Supercurrent enhancement in Bloch domain walls. *Sci. Rep.* **2**, 699; DOI:10.1038/srep00699 (2012).